Since January 2020 Elsevier has created a COVID-19 resource centre with free information in English and Mandarin on the novel coronavirus COVID-19. The COVID-19 resource centre is hosted on Elsevier Connect, the company's public news and information website.

Elsevier hereby grants permission to make all its COVID-19-related research that is available on the COVID-19 resource centre - including this research content - immediately available in PubMed Central and other publicly funded repositories, such as the WHO COVID database with rights for unrestricted research re-use and analyses in any form or by any means with acknowledgement of the original source. These permissions are granted for free by Elsevier for as long as the COVID-19 resource centre remains active.

Informatics in Medicine Unlocked 32 (2022) 101028

Contents lists available at ScienceDirect

Informatics in Medicine Unlocked

journal homepage: www.elsevier.com/locate/imu

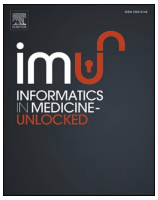

Artificial neural network-based heuristic to solve COVID-19 model including government strategies and individual responses

Thongchai Botmart [a], Zulqurnain Sabir [b], Shumaila Javeed [c], Rafaél Artidoro Sandoval Núñez [d], Wajaree weera [a], Mohamed R. Ali [e,*], R. Sadat [f]

[a] Department of Mathematics, Faculty of Science, Khon Kaen University, Khon Kaen, 40002, Thailand
[b] Department of Mathematics and Statistics, Hazara University, Mansehra, Pakistan
[c] Department of Mathematics, COMSATS University Islamabad, Pakistan
[d] Universidad Nacional Autónoma de Chota, Cajamarca, Peru
[e] Faculty of Engineering and Technology, Future University, Cairo, Egypt
[f] Department of Mathematics, Zagazig Faculty of Engineering, Zagazig University, Egypt

ARTICLE INFO

Keywords:
Spread of COVID-19
Nonlinear SEIR-NDC model
Artificial neural networks
Active-set
Genetic algorithm

ABSTRACT

The current work aims to design a computational framework based on artificial neural networks (ANNs) and the optimization procedures of global and local search approach to solve the nonlinear dynamics of the spread of COVID-19, i.e., the SEIR-NDC model. The combination of the Genetic algorithm (GA) and active-set approach (ASA), i.e., GA-ASA, works as a global-local search scheme to solve the SEIR-NDC model. An error-based fitness function is optimized through the hybrid combination of the GA-ASA by using the differential SEIR-NDC model and its initial conditions. The numerical performances of the SEIR-NDC nonlinear model are presented through the procedures of ANNs along with GA-ASA by taking ten neurons. The correctness of the designed scheme is observed by comparing the obtained results based on the SEIR-NDC model and the reference Adams method. The absolute error performances are performed in suitable ranges for each dynamic of the SEIR-NDC model. The statistical analysis is provided to authenticate the reliability of the proposed scheme. Moreover, performance indices graphs and convergence measures are provided to authenticate the exactness and constancy of the proposed stochastic scheme.

1. Introduction

The progress of science based on technology and material has been highly demanded in recent years. However, there are various obstacles to encounter hardly in daily life. For example, a novel coronavirus is one of the most dangerous viruses humans have attacked since 2020. This virus transmits rapidly from human to human, and now it has spread worldwide. Millions of people have died from this virus, and many positive cases have been reported with high recovery rates [1–5]. The common symptoms of coronavirus are sore throats, coughs, fever, and headaches, as well as some other respiratory indications, like high temperature, even bleeding, phlegm, chest pain, and breath shortness [6–9].

Recently, the researcher's community has taken a keen interest in investigating the dynamics of COVID-19. Donders et al. [10] presented the ISIDOG recommendations related to COVID-19 and pregnancy. Wang [11] designed a model for coronavirus using the applications, confines, and capacities. Rhodes et al. [12] presented a mathematical model of public troubles in COVID-19 infection control. Jewell et al. [13] showed the potential effects of disruption to HIV programs in sub-Saharan Africa caused by COVID-19. Khrapov et al. [14] expressed the comparative analysis of the mathematical models based on the dynamics of the coronavirus COVID-19 epidemic development in different countries. Thompson [15] constructed epidemiological models, considered essential tools for guiding COVID-19 interventions. Sánchez et al. [16] proposed a SITR fractal nonlinear dynamics of a novel COVID-19. Elsonbaty et al. [17] analyzed the discrete fractional SITRs model for COVID-19. Umer et al. [18,19] presented the numerical solutions using the heuristic and swarming approaches based on the SITR model.

Various areas involve mathematical models, like health, biology, physics, chemistry, civil/mechanical engineering, and economics.

* Corresponding author.
E-mail addresses: asandoval@unach.edu.pe (R.A. Sandoval Núñez), Mohamed.Reda@fue.edu.eg (M.R. Ali).

https://doi.org/10.1016/j.imu.2022.101028
Received 3 June 2022; Received in revised form 15 July 2022; Accepted 16 July 2022
Available online 6 August 2022
2352-9148/© 2022 Published by Elsevier Ltd. This is an open access article under the CC BY-NC-ND license (http://creativecommons.org/licenses/by-nc-nd/4.0/).

Kharis and Kholisoh stated that mathematical science plays a crucial role in preventing the spread of illness [20]. A mathematical form of the model can be implemented to investigate the spread of viruses. Yulida stated that mathematics had a significant part in exploring the disease outbreak, spreading, and predicting designs known as epidemiology [21]. For the numerical outcomes of these models, the stochastic solvers based on the artificial neural networks (ANNs) together with the optimization procedures of global/local search approaches based on genetic algorithm (GA) and active-set approach (ASA), i.e., GA-ASA has been implemented for solving the spreading of coronavirus, i.e., SEIR-NDC model. The stochastic approaches of ANNs under the optimization procedures of the GA-ASA have never been implemented to solve the SEIR-NDC model. Some well-known applications of the stochastic procedures are the delay differential singular systems [22,23], prey-predator system [24], fractional singular models [25–27], HIV infection system [28], corneal shape models [29,30], functional differential models [31], Thomas-Fermi differential model [32], mosquito dispersal system [33], heat conduction model [34] and periodic form of the singular models [35,36].

The SEIR-NDC nonlinear mathematical model depends upon seven categories, susceptible (S), exposed population (E), infected people (I), removed individuals (R), total population (N), public observation (D), and cumulative (C), which are given as [37]:

i

$$\begin{cases} \frac{dS(\aleph)}{d\aleph} = -\frac{\beta_0 E(\aleph)S(\aleph)}{N} - \frac{\beta(\aleph)I(\aleph)S(\aleph)}{N} - \mu S(\aleph), S(0) = i_1, \\ \frac{dE(\aleph)}{d\aleph} = \frac{\beta_0 E(\aleph)S(\aleph)}{N} + \frac{\beta(\aleph)I(\aleph)S(\aleph)}{N} - (\mu+\sigma)E(\aleph), E(0) = i_2, \\ \frac{dI(\aleph)}{d\aleph} = \sigma E(\aleph) - (\mu+\gamma)I(\aleph), I(0) = i_3, \\ \frac{dR(\aleph)}{d\aleph} = -\mu R(\aleph) + \gamma I(\aleph), R(0) = i_4, \\ \frac{dN(\aleph)}{d\aleph} = -\mu N(\aleph), \quad N(0) = i_5, \\ \frac{dD(\aleph)}{d\aleph} = -\lambda D(\aleph) + d\gamma I(\aleph), \quad D(0) = i_6, \\ \frac{dC(\aleph)}{d\aleph} = \sigma E(\aleph), \quad C(0) = i_7. \end{cases} \tag{1}$$

where μ, σ, β_0, $\beta(\aleph)$, γ, λ and d indicate the relocation rate, latent, pr mary transmission rate, transmission rate at time $\aleph$, infected, public response and severe case values. The initial conditions (ICs) are i_1, i_2, i_3, i_4, i_5, i_6 and i_7. Some novel features of the ANNs by using the optimization procedures of GA-ASA are provided:

- The solution of the SEIR-NDC-based COVID-19 model is effectively presented by using the stochastic computational heuristic-based ANNs along with the optimization procedures of GA-ASA.
- The performances through ANNs with the optimization-based stochastic procedures are testified by matching the proposed and reference results.
- The absolute error (AE) values lie in suitable ranges to solve the SEIR-NDC model, which presents the worth of the stochastic computational performances.
- The consistency of the proposed computational heuristic-based ANNs, along with the optimization procedures of GA-ASA, is realistic by applying the statistical measures on multiple runs to solve the nonlinear SEIR-NDC model.
- The statistical performances based on Theil's inequality coefficient (TIC), variance account for (VAF), and mean absolute deviation (MAD) have been used to perform the solutions of the SEIR-NDC model.

The paper is organized as follows: Sect 2 performs the proposed results. Sect 3 provides the performance catalogs. Section 4 presents the results and detailed discussions of the nonlinear SEIR-NDC model. The final remarks are listed in the final Sect.

2. Methodology

In this section, the proposed ANNs and the optimization procedures of GA-ASA are presented in two phases to find the numerical results of the nonlinear SEIR-NDC model. In addition, the introduction of an error-based fitness function and the optimization-based procedural steps of GA-ASA are also presented.

2.1. ANN modeling

The mathematical formulations given in the system (1), along with the derivative performances, are provided:

$$\begin{bmatrix} \widehat{S}(\aleph), \widehat{E}(\aleph), \\ \widehat{I}(\aleph), \widehat{R}(\aleph), \\ \widehat{N}(\aleph), \widehat{D}(\aleph) \\ \widehat{C}(\aleph) \end{bmatrix} = \begin{bmatrix} \sum_{k=1}^{m} z_{S,k} L\left(w_{S,k}\aleph + p_{S,k}\right), & \sum_{k=1}^{m} z_{E,k} L\left(w_{E,k}\aleph + p_{E,k}\right), \\ \sum_{k=1}^{m} z_{I,k} L\left(w_{I,k}\aleph + p_{I,k}\right), & \sum_{k=1}^{m} z_{R,k} L\left(w_{R,k}\aleph + p_{R,k}\right), \\ \sum_{k=1}^{m} z_{N,k} L\left(w_{N,k}\aleph + p_{N,k}\right), & \sum_{k=1}^{m} z_{D,k} L\left(w_{D,k}\aleph + p_{D,k}\right), \\ \sum_{k=1}^{m} z_{C,k} L\left(w_{C,k}\aleph + p_{C,k}\right), \end{bmatrix}, \tag{2}$$

$$\begin{bmatrix} \frac{d\widehat{S}}{d\aleph}, \frac{d\widehat{E}}{d\aleph}, \\ \frac{d\widehat{I}}{d\aleph}, \frac{d\widehat{R}}{d\aleph}, \\ \frac{d\widehat{N}}{d\aleph}, \frac{d\widehat{D}}{d\aleph} \\ \frac{d\widehat{C}}{d\aleph} \end{bmatrix} = \begin{bmatrix} \sum_{k=1}^{m} z_{S,k} \frac{d}{d\aleph} L\left(w_{S,k}\aleph + p_{S,k}\right), & \sum_{k=1}^{m} z_{E,k} \frac{d}{d\aleph} L\left(w_{E,k}\aleph + p_{E,k}\right), \\ \sum_{k=1}^{m} z_{I,k} \frac{d}{d\aleph} L\left(w_{I,k}\aleph + p_{I,k}\right), & \sum_{k=1}^{m} z_{R,k} \frac{d}{d\aleph} L\left(w_{R,k}\aleph + p_{R,k}\right), \\ \sum_{k=1}^{m} z_{N,k} \frac{d}{d\aleph} L\left(w_{N,k}\aleph + p_{N,k}\right), & \sum_{k=1}^{m} z_{D,k} \frac{d}{d\aleph} L\left(w_{D,k}\aleph + p_{D,k}\right), \\ \sum_{k=1}^{m} z_{C,k} \frac{d}{d\aleph} L\left(w_{C,k}\aleph + p_{C,k}\right), \end{bmatrix}.$$

Where, the unknown weight vector is $\boldsymbol{W}$, which is given:

$$\boldsymbol{W} = \begin{bmatrix} \boldsymbol{W}_S \\ \boldsymbol{W}_E \\ \boldsymbol{W}_I \\ \boldsymbol{W}_R \\ \boldsymbol{W}_N \\ \boldsymbol{W}_D \\ \boldsymbol{W}_C \end{bmatrix}^t, \text{ where } \boldsymbol{W}_S = \begin{bmatrix} \boldsymbol{z}_S \\ \boldsymbol{w}_S \\ \boldsymbol{p}_S \end{bmatrix}^t, \boldsymbol{W}_E = \begin{bmatrix} \boldsymbol{z}_E \\ \boldsymbol{w}_E \\ \boldsymbol{p}_E \end{bmatrix}^t, \boldsymbol{W}_I = \begin{bmatrix} \boldsymbol{z}_I \\ \boldsymbol{w}_I \\ \boldsymbol{p}_I \end{bmatrix}^t, \boldsymbol{W}_R = \begin{bmatrix} \boldsymbol{z}_R \\ \boldsymbol{w}_R \\ \boldsymbol{p}_R \end{bmatrix}^t, \boldsymbol{W}_N = \begin{bmatrix} \boldsymbol{z}_N \\ \boldsymbol{w}_N \\ \boldsymbol{p}_N \end{bmatrix}^t, \boldsymbol{W}_D = \begin{bmatrix} \boldsymbol{z}_D \\ \boldsymbol{w}_D \\ \boldsymbol{p}_D \end{bmatrix}^t \text{ and } \boldsymbol{W}_C = \begin{bmatrix} \boldsymbol{z}_C \\ \boldsymbol{w}_C \\ \boldsymbol{p}_C \end{bmatrix}^t$$

Table 1
Description of the stochastic procedure for the nonlinear SEIR-NDC system.

Optimization of the [GA] procedure

[Inputs]: For the same elements, the chromosomes are indicated as: $\boldsymbol{W} = [\boldsymbol{z}, \boldsymbol{w}, \boldsymbol{p}]$

[Population]: The representations of the chromosome set is provided as:

$$\boldsymbol{W} = \begin{bmatrix} \boldsymbol{W}_S \\ \boldsymbol{W}_E \\ \boldsymbol{W}_I \\ \boldsymbol{W}_R \\ \boldsymbol{W}_N \\ \boldsymbol{W}_D \\ \boldsymbol{W}_C \end{bmatrix}^t, \text{ where } \boldsymbol{W}_S = \begin{bmatrix} \boldsymbol{z}_S \\ \boldsymbol{w}_S \\ \boldsymbol{p}_S \end{bmatrix}^t, \boldsymbol{W}_E = \begin{bmatrix} \boldsymbol{z}_E \\ \boldsymbol{w}_E \\ \boldsymbol{p}_E \end{bmatrix}^t, \boldsymbol{W}_I = \begin{bmatrix} \boldsymbol{z}_I \\ \boldsymbol{w}_I \\ \boldsymbol{p}_I \end{bmatrix}^t, \boldsymbol{W}_R = \begin{bmatrix} \boldsymbol{z}_R \\ \boldsymbol{w}_R \\ \boldsymbol{p}_R \end{bmatrix}^t, \boldsymbol{W}_N = \begin{bmatrix} \boldsymbol{z}_N \\ \boldsymbol{w}_N \\ \boldsymbol{p}_N \end{bmatrix}^t,$$

$$\boldsymbol{W}_D = \begin{bmatrix} \boldsymbol{z}_D \\ \boldsymbol{w}_D \\ \boldsymbol{p}_D \end{bmatrix}^t \text{ and } \boldsymbol{W}_C = \begin{bmatrix} \boldsymbol{z}_C \\ \boldsymbol{w}_C \\ \boldsymbol{p}_C \end{bmatrix}^t$$

[Output]: Global best vectors = $W_{\text{GA-Best}}$

Initialization: For the collection of the chromosomes, specify the $\boldsymbol{W}_{\textbf{GA-Best}}$ values.

[Fitness Assessment]: Modify the values of the Fitness (ξ_F) through the population [***P***] for Eqs 4-12.

- **[Stopping values]:** Stop the procedure, when the below criteria meet, [Generations = 60], [TolCon =10^{-20}], [ξ_F = 10^{-22}], [StallLimit=150], [TolFun = 10^{-21}] & [PopSize=180]

Now, go to [**storage]**

[Ranking]: $\boldsymbol{W}_{\textbf{GA-Best}}$ is the rank in *P*.

[Storage]: [$\boldsymbol{W}_{\textbf{GA-Best}}$], ξ_F,[time], [Epochs] & [function count] for GA.

End of [GA] procedure

Starts of the [ASA] procedure

[Inputs]: Starting point = $\boldsymbol{W}_{\textbf{GA-Best}}$.

[Output]: Best weights of GA-ASA are $\boldsymbol{W}_{\textbf{GA-ASA}}$.

[Initialize]: Iterations $\boldsymbol{W}_{\textbf{GA-Best}}$ & Projects.

[Terminating values]: [Iterations = 150], ξ_F = 10^{-20}], [TolX = 10^{-19}], [[MaxFunEvals= 221000] & [TolFun = 10^{-21}].

[Approximation of FIT]: Calculate [$\boldsymbol{W}_{\textbf{GA-ASA}}$] and ξ_F for Eqs. 4-12.

[Amendments]: [fmincon] for ASA, and ξ_F

[Store]: Transform [$\boldsymbol{W}_{\textbf{GA-ASA}}$], ξ_F, [time], [generations], and count of functions.

End of [ASA] Procedure

$$\boldsymbol{z}_S = \left[z_{S,1},\ z_{S,2},\ z_{S,3},\ldots,z_{S,m}\right],\quad \boldsymbol{z}_E = \left[z_{E,1},\ z_{E,2},\ z_{E,3},\ldots,z_{E,m}\right],\quad \boldsymbol{z}_I = \left[z_{I,1},\ z_{I,2},\ z_{I,3},\ldots,z_{I,m}\right],$$
$$\boldsymbol{z}_R = \left[z_{R,1},\ z_{R,2},\ z_{R,3},\ldots,z_{R,m}\right],\quad \boldsymbol{z}_N = \left[z_{N,1},\ z_{N,2},\ z_{N,3},\ldots,z_{N,m}\right],\quad \boldsymbol{z}_D = \left[z_{D,1},\ z_{D,2},\ z_{D,3},\ldots,z_{D,m}\right],$$
$$\boldsymbol{z}_C = \left[z_{C,1},\ z_{C,2},\ z_{C,3},\ldots,z_{C,m}\right],\quad \boldsymbol{w}_S = \left[w_{S,1},\ w_{S,2},\ w_{S,3},\ldots,w_{S,m}\right],\ \boldsymbol{w}_E = \left[w_{E,1},\ w_{E,2},\ w_{E,3},\ldots,w_{E,m}\right],$$
$$\boldsymbol{w}_I = \left[w_{I,1},\ w_{I,2},\ w_{I,3},\ldots,w_{I,m}\right],\ \boldsymbol{w}_R = \left[w_{R,1},\ w_{R,2},\ w_{R,3},\ldots,w_{R,m}\right],\quad \boldsymbol{w}_N = \left[w_{N,1},w_{N,2},w_{N,3},\ldots,\ w_{N,m}\right],$$
$$\boldsymbol{w}_D = \left[w_{D,1},w_{D,2},w_{D,3},\ldots,\ w_{D,m}\right],\quad \boldsymbol{w}_C = \left[w_{C,1},w_{C,2},w_{C,3},\ldots,\ w_{C,m}\right],\quad \boldsymbol{p}_S = \left[p_{S,1},\ p_{S,2},\ p_{S,3},\ldots,p_{S,m}\right],$$
$$\boldsymbol{p}_E = \left[p_{E,1},\ p_{E,2},\ p_{E,3},\ldots,p_{E,m}\right],\quad \boldsymbol{p}_I = \left[p_{I,1},\ p_{I,2},\ p_{I,3},\ldots,p_{I,m}\right],\quad \boldsymbol{p}_R = \left[p_{R,1},\ p_{R,2},\ p_{R,3},\ldots,p_{R,m}\right],$$
$$\boldsymbol{p}_N = \left[p_{N,1},\ p_{N,2},\ p_{N,3},\ldots,p_{N,m}\right],\ \boldsymbol{p}_D = \left[p_{D,1},\ p_{D,2},\ p_{D,3},\ldots,p_{D,m}\right],\ \boldsymbol{p}_C = \left[p_{C,1},\ p_{C,2},\ p_{C,3},\ldots,p_{C,m}\right],$$

An activation log-sigmoid function is applied in this study [38,39], the mathematical form of the log-sigmoid function is given: $L(\aleph) = (1+\exp(-\aleph))^{-1}$.

$$\begin{bmatrix}\widehat{S}(\aleph),\ \widehat{E}(\aleph),\ \widehat{I}(\aleph),\\ \widehat{R}(\aleph),\widehat{N}(\aleph),\widehat{D}(\aleph),\\ \widehat{C}(\aleph)\end{bmatrix} = \begin{bmatrix}\sum_{k=1}^{m}\frac{z_{S,k}}{1+e^{-\left(w_{S,k}\aleph+p_{S,k}\right)}},\ \sum_{k=1}^{m}\frac{z_{E,k}}{1+e^{-\left(w_{E,k}\aleph+p_{E,k}\right)}},\ \sum_{k=1}^{m}\frac{z_{I,k}}{1+e^{-\left(w_{I,k}\aleph+p_{I,k}\right)}},\\ \sum_{k=1}^{m}\frac{z_{R,k}}{1+e^{-\left(w_{R,k}\aleph+p_{R,k}\right)}},\sum_{k=1}^{m}\frac{z_{N,k}}{1+e^{-\left(w_{N,k}\aleph+p_{N,k}\right)}},\ \sum_{k=1}^{m}\frac{z_{D,k}}{1+e^{-\left(w_{D,k}\aleph+p_{D,k}\right)}},\\ \sum_{k=1}^{m}\frac{z_{C,k}}{1+e^{-\left(w_{C,k}\aleph+p_{C,k}\right)}},\end{bmatrix},$$

$$\begin{bmatrix}\frac{d\widehat{S}}{d\aleph},\ \frac{d\widehat{E}}{d\aleph},\frac{d\widehat{I}}{d\aleph},\\ \frac{d\widehat{R}}{d\aleph},\ \frac{d\widehat{N}}{d\aleph},\frac{d\widehat{D}}{d\aleph},\\ \frac{d\widehat{C}}{d\aleph}\end{bmatrix} = \begin{bmatrix}\sum_{k=1}^{m}\frac{w_{S,k}z_{S,k}e^{-\left(w_{S,k}\aleph+p_{S,k}\right)}}{\left(1+e^{-\left(w_{S,k}\aleph+p_{S,k}\right)}\right)^2},\ \sum_{k=1}^{m}\frac{w_{E,k}z_{E,k}e^{-\left(w_{E,k}\aleph+p_{E,k}\right)}}{\left(1+e^{-\left(w_{E,k}\aleph+p_{E,k}\right)}\right)^2},\\ \sum_{k=1}^{m}\frac{w_{I,k}z_{I,k}e^{-\left(w_{I,k}\aleph+p_{I,k}\right)}}{\left(1+e^{-\left(w_{I,k}\aleph+p_{I,k}\right)}\right)^2},\quad \sum_{k=1}^{m}\frac{w_{R,k}z_{R,k}e^{-\left(w_{R,k}\aleph+p_{R,k}\right)}}{\left(1+e^{-\left(w_{R,k}\aleph+p_{R,k}\right)}\right)^2},\\ \sum_{k=1}^{m}\frac{w_{N,k}z_{N,k}e^{-\left(w_{N,k}\aleph+p_{N,k}\right)}}{\left(1+e^{-\left(w_{N,k}\aleph+p_{N,k}\right)}\right)^2},\quad \sum_{k=1}^{m}\frac{w_{D,k}z_{D,k}e^{-\left(w_{D,k}\aleph+p_{D,k}\right)}}{\left(1+e^{-\left(w_{D,k}\aleph+p_{D,k}\right)}\right)^2},\\ \sum_{k=1}^{m}\frac{w_{C,k}z_{R,k}e^{-\left(w_{C,k}\aleph+p_{C,k}\right)}}{\left(1+e^{-\left(w_{C,k}\aleph+p_{C,k}\right)}\right)^2}\end{bmatrix}. \tag{3}$$

The error function is given:

$$\xi_F = \xi_{F1}+\xi_{F2}+\xi_{F3}+\xi_{F4}+\xi_{F5}+\xi_{F6}+\xi_{F7}+\xi_{F8}, \tag{4}$$

$$\xi_{F1} = \frac{1}{N}\sum_{k=1}^{N}\left(\frac{d\widehat{S}}{d\aleph_k}+\frac{\beta_0\widehat{E}_k\widehat{S}_k}{N}+\frac{\beta(\aleph_k)\widehat{I}_k\widehat{S}_k}{N}+\mu\widehat{S}_k\right)^2, \tag{5}$$

$$\xi_{F2} = \frac{1}{N}\sum_{k=1}^{N}\left(\frac{d\widehat{E}}{d\aleph_k}-\frac{\beta_0\widehat{E}_k\widehat{S}_k}{N}-\frac{\beta(\aleph_k)\widehat{I}_k\widehat{S}_k}{N}+\mu\widehat{E}_k+\sigma\widehat{E}_k\right)^2, \tag{6}$$

$$\xi_{F3} = \frac{1}{N}\sum_{k=1}^{N}\left(\frac{d\widehat{I}}{d\aleph_k}+\gamma\widehat{I}_k+\mu\widehat{I}_k-\sigma\widehat{E}_k\right)^2, \tag{7}$$

$$\xi_{F4} = \frac{1}{N}\sum_{k=1}^{N}\left(\frac{d\widehat{R}}{d\aleph_k}-\gamma\widehat{I}_k+\mu\widehat{R}_k\right)^2, \tag{8}$$

$$\xi_{F5} = \frac{1}{N}\sum_{k=1}^{N}\left(\frac{d\widehat{N}}{d\aleph_k}+\mu\widehat{N}_k\right)^2, \tag{9}$$

$$\xi_{F6} = \frac{1}{N}\sum_{k=1}^{N}\left(\frac{d\widehat{D}}{d\aleph_k}+\lambda\widehat{D}_k-d\gamma\widehat{I}_k\right)^2, \tag{10}$$

$$\xi_{F7} = \frac{1}{N}\sum_{k=1}^{N}\left(\frac{d\widehat{C}}{d\aleph_k}-\sigma\widehat{E}_k\right)^2, \tag{11}$$

$$\xi_{F8} = \frac{1}{7}\left((\widehat{S}_0-i_1)^2+(\widehat{E}_0-i_2)^2+(\widehat{I}_0-i_3)^2+(\widehat{R}_0-i_4)^2+(\widehat{N}_0-i_5)^2+(\widehat{D}_0-i_6)^2+(\widehat{C}_0-i_7)^2\right), \tag{12}$$

where $\aleph_k = kh$, $\widehat{S}_k = \widehat{S}(\aleph_k), \widehat{I}_k = \widehat{I}(\aleph_k), \widehat{E}_k = \widehat{E}(\aleph_k), \widehat{R}_k = \widehat{R}(\aleph_k), \widehat{N}_k = \widehat{N}(\aleph_k)$, $\widehat{D}_k = \widehat{D}(\aleph_k), \widehat{C}_k = \widehat{C}(\aleph_k)$ and $Nh = 1$. The proposed solutions of the nonlinear SEIR-NDC model are $\widehat{S}_k = \widehat{S}(\aleph_k), \widehat{I}_k = \widehat{I}(\aleph_k), \widehat{E}_k = \widehat{E}(\aleph_k), \widehat{R}_k = \widehat{R}(\aleph_k), \widehat{N}_k = \widehat{N}(\aleph_k), \widehat{D}_k = \widehat{D}(\aleph_k)$ and $\widehat{C}_k = \widehat{C}(\aleph_k)$. Likewise, $\xi_{F1}, \xi_{F2}, \xi_{F3}, \xi_{F4}, \xi_{F5}, \xi_{F6}, \xi_{F7}$ and ξ_{F8} are the merit functions based differential SEIR-NDC model and its ICs.

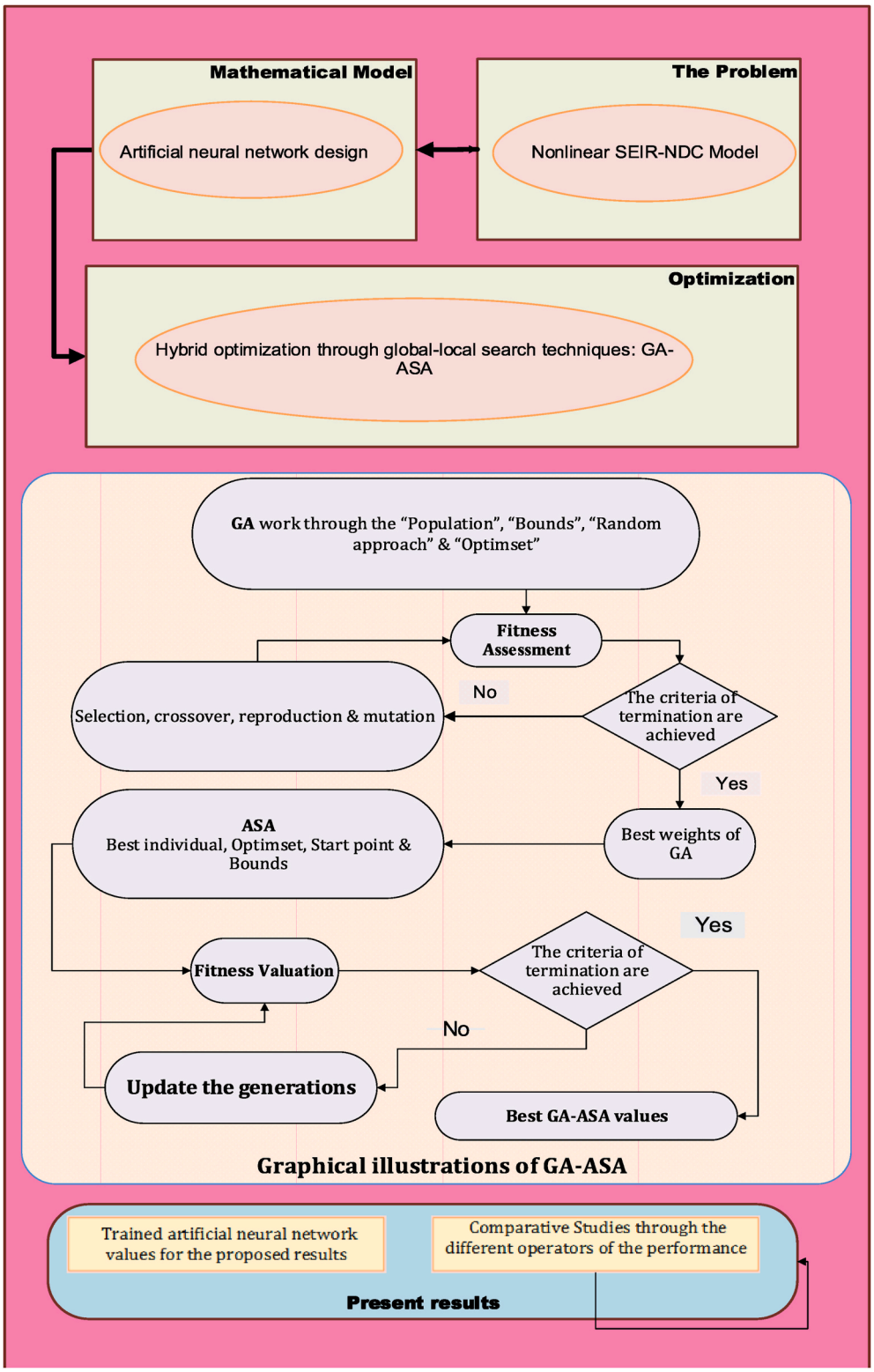

Fig. 1. The proposed scheme GA-ASA structure for the SEIR-NDC system.

2.2. Optimization performance: GA-ASA

This section provides the details of the global and local search methods based on the GA and ASA for the SEIR-NDC system based on COVID-19. The global search GA is an optimization scheme to solve the constrained/unconstrained equations. GA is an optimization procedure that is used to apply the "crossover," "selection," "mutation," and "elitism" procedures. Recently, GA has been used in cancer, lung prediction [40], pupils' academic performance prediction [41], wellhead back based pressure control model [42], mutation for the test data generation systems [43], bearing accountability analysis of induction motors [44], optimization of human resources in sanitorium emergency [45], sensor acquisition frequency [46], singular nonlinear model [47] and automated manufacturing networks [48].

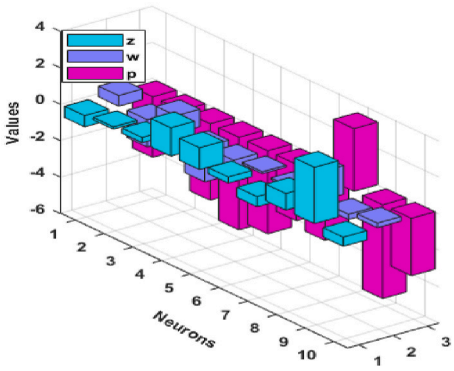

(a): Best weights: $\hat{S}(\aleph)$

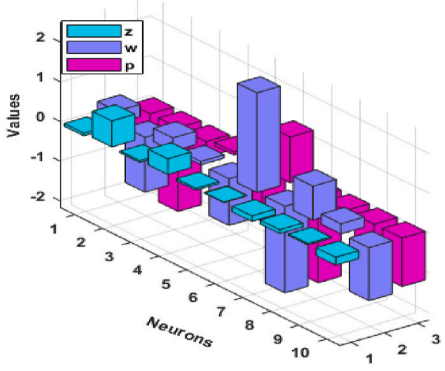

(b): Best weights: $\hat{E}(\aleph)$

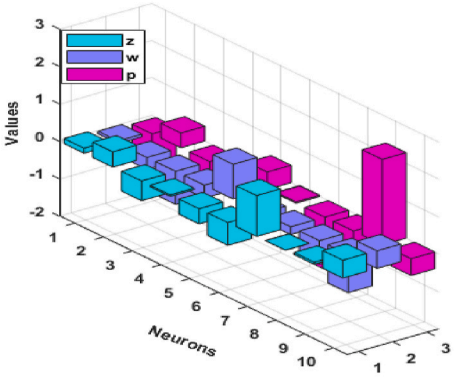

(c): Best weights: $\hat{I}(\aleph)$

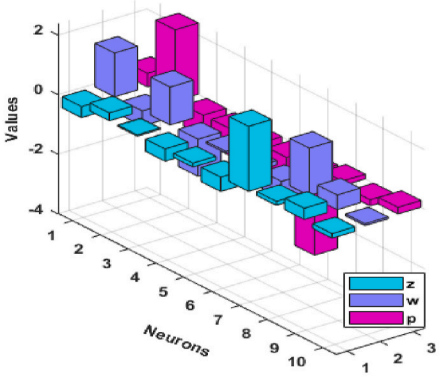

(d): Best weights: $\hat{R}(\aleph)$

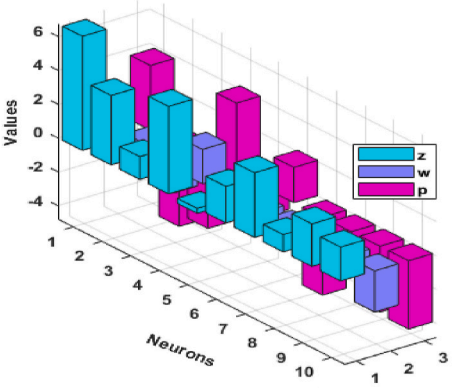

(e): Best weights: $\hat{N}(\aleph)$

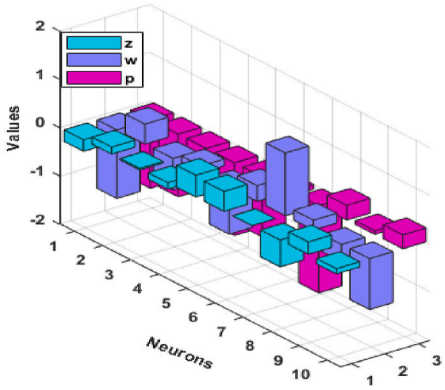

(f): Best weights: $\hat{D}(\aleph)$

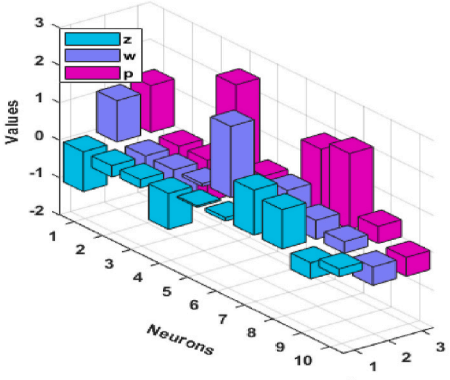

(g): Best weights: $\hat{C}(\aleph)$

Fig. 2. Best weight vectors for the nonlinear SEIR-NDC model.

The hybridization of the GA is performed with the local search approach by taking GA best values as an initial input to find the rapid performances. In this regard, an operative ASA is executed to regulate the consequences and GA procedure using optimization. In recent decades, ASA has been implemented in large-scale optimization systems, including box constraints [49], cardiac defibrillation [50], regularized monotonic regression [51], predictive switch for a beam and ball system [52], and multivariate integration through the uncertain error demand [53]. The current work is linked to solving the nonlinear SEIR-NDC system through the GA-ASA optimization procedures. The inclusive descriptions of the stochastic procedures are listed in Table 1.

$$\begin{bmatrix} \mathrm{TIC}_S, \mathrm{TIC}_E, \mathrm{TIC}_I, \\ \mathrm{TIC}_R, \mathrm{TIC}_N, \mathrm{TIC}_D, \\ \mathrm{TIC}_C \end{bmatrix} = \begin{bmatrix} \dfrac{\sqrt{\frac{1}{n}\sum_{k=1}^{n}(S_k-\widehat{S}_k)^2}}{\left(\sqrt{\frac{1}{n}\sum_{k=1}^{n}S_k^2}+\sqrt{\frac{1}{n}\sum_{k=1}^{n}\widehat{S}_k^2}\right)}, & \dfrac{\sqrt{\frac{1}{n}\sum_{k=1}^{n}(E_k-\widehat{E}_k)^2}}{\left(\sqrt{\frac{1}{n}\sum_{k=1}^{n}E_k^2}+\sqrt{\frac{1}{n}\sum_{k=1}^{n}\widehat{E}_k^2}\right)}, \\ \dfrac{\sqrt{\frac{1}{n}\sum_{k=1}^{n}(I_k-\widehat{I}_k)^2}}{\left(\sqrt{\frac{1}{n}\sum_{k=1}^{n}I_k^2}+\sqrt{\frac{1}{n}\sum_{k=1}^{n}\widehat{I}_k^2}\right)}, & \dfrac{\sqrt{\frac{1}{n}\sum_{k=1}^{n}(R_k-\widehat{R}_k)^2}}{\left(\sqrt{\frac{1}{n}\sum_{k=1}^{n}R_k^2}+\sqrt{\frac{1}{n}\sum_{k=1}^{n}\widehat{R}_k^2}\right)}, \\ \dfrac{\sqrt{\frac{1}{n}\sum_{k=1}^{n}(N_k-\widehat{N}_k)^2}}{\left(\sqrt{\frac{1}{n}\sum_{k=1}^{n}N_k^2}+\sqrt{\frac{1}{n}\sum_{k=1}^{n}\widehat{N}_k^2}\right)}, & \dfrac{\sqrt{\frac{1}{n}\sum_{k=1}^{n}(D_k-\widehat{D}_k)^2}}{\left(\sqrt{\frac{1}{n}\sum_{k=1}^{n}\widehat{D}_k^2}+\sqrt{\frac{1}{n}\sum_{k=1}^{n}\widehat{D}_k^2}\right)}, \\ \dfrac{\sqrt{\frac{1}{n}\sum_{k=1}^{n}(C_k-\widehat{C}_k)^2}}{\left(\sqrt{\frac{1}{n}\sum_{k=1}^{n}\widehat{C}_k^2}+\sqrt{\frac{1}{n}\sum_{k=1}^{n}\widehat{C}_k^2}\right)} & \end{bmatrix}, \tag{13}$$

$$\begin{cases} \begin{bmatrix} \mathrm{VAF}_S, \mathrm{VAF}_E, \\ \mathrm{VAF}_I, \mathrm{VAF}_R, \\ \mathrm{VAF}_N, \ \mathrm{VAF}_D, \\ \mathrm{VAF}_C \end{bmatrix} = \begin{bmatrix} \left(1-\dfrac{\mathrm{var}(S_k-\widehat{S}_k)}{\mathrm{var}(S_k)}\right)\times 100, & \left(1-\dfrac{\mathrm{var}(E_k-\widehat{E}_k)}{\mathrm{var}(E_k)}\right)\times 100, \\ \left(1-\dfrac{\mathrm{var}(I_k-\widehat{I}_k)}{\mathrm{var}(I_k)}\right)\times 100, & \left(1-\dfrac{\mathrm{var}(R_k-\widehat{R}_k)}{\mathrm{var}(R_k)}\right)\times 100, \\ \left(1-\dfrac{\mathrm{var}(N_k-\widehat{N}_k)}{\mathrm{var}(N_k)}\right)\times 100, & \left(1-\dfrac{\mathrm{var}(D_k-\widehat{D}_k)}{\mathrm{var}(D_k)}\right)\times 100, \\ \left(1-\dfrac{\mathrm{var}(C_k-\widehat{C}_k)}{\mathrm{var}(C_k)}\right)\times 100, & \end{bmatrix} \\ \begin{bmatrix} \mathrm{EVAF}_S, \mathrm{EVAF}_E, \mathrm{EVAF}_I, \\ \mathrm{EVAF}_R, \mathrm{EVAF}_N, \ \mathrm{EVAF}_D, \\ \mathrm{EVAF}_C \end{bmatrix} = \begin{bmatrix} 100-\mathrm{VAF}_S, 100-\mathrm{VAF}_E, 100-\mathrm{VAF}_I, \\ 100-\mathrm{VAF}_R, 100-\mathrm{VAF}_N, 100-\mathrm{VAF}_D, \\ 100-\mathrm{VAF}_C \end{bmatrix}, \end{cases} \tag{14}$$

$$\begin{bmatrix} \mathrm{MAD}_S, \mathrm{MAD}_E, \mathrm{MAD}_I, \\ \mathrm{MAD}_R, \mathrm{MAD}_N, \mathrm{MAD}_D, \\ \mathrm{MAD}_C \end{bmatrix} = \begin{bmatrix} \frac{1}{n}\sum_{k=1}^{n}|(S_k-\widehat{S}_k)|, & \frac{1}{n}\sum_{k=1}^{n}|(E_k-\widehat{E}_k)|, & \frac{1}{n}\sum_{k=1}^{n}|(I_k-\widehat{I}_k)|, \\ \frac{1}{n}\sum_{k=1}^{n}|(R_k-\widehat{R}_k)|, & \frac{1}{n}\sum_{k=1}^{n}|(N_k-\widehat{N}_k)|, & \frac{1}{n}\sum_{k=1}^{n}|(D_k-\widehat{D}_k)|, \\ \frac{1}{n}\sum_{k=1}^{n}|(C_k-\widehat{C}_k)| & & \end{bmatrix}. \tag{15}$$

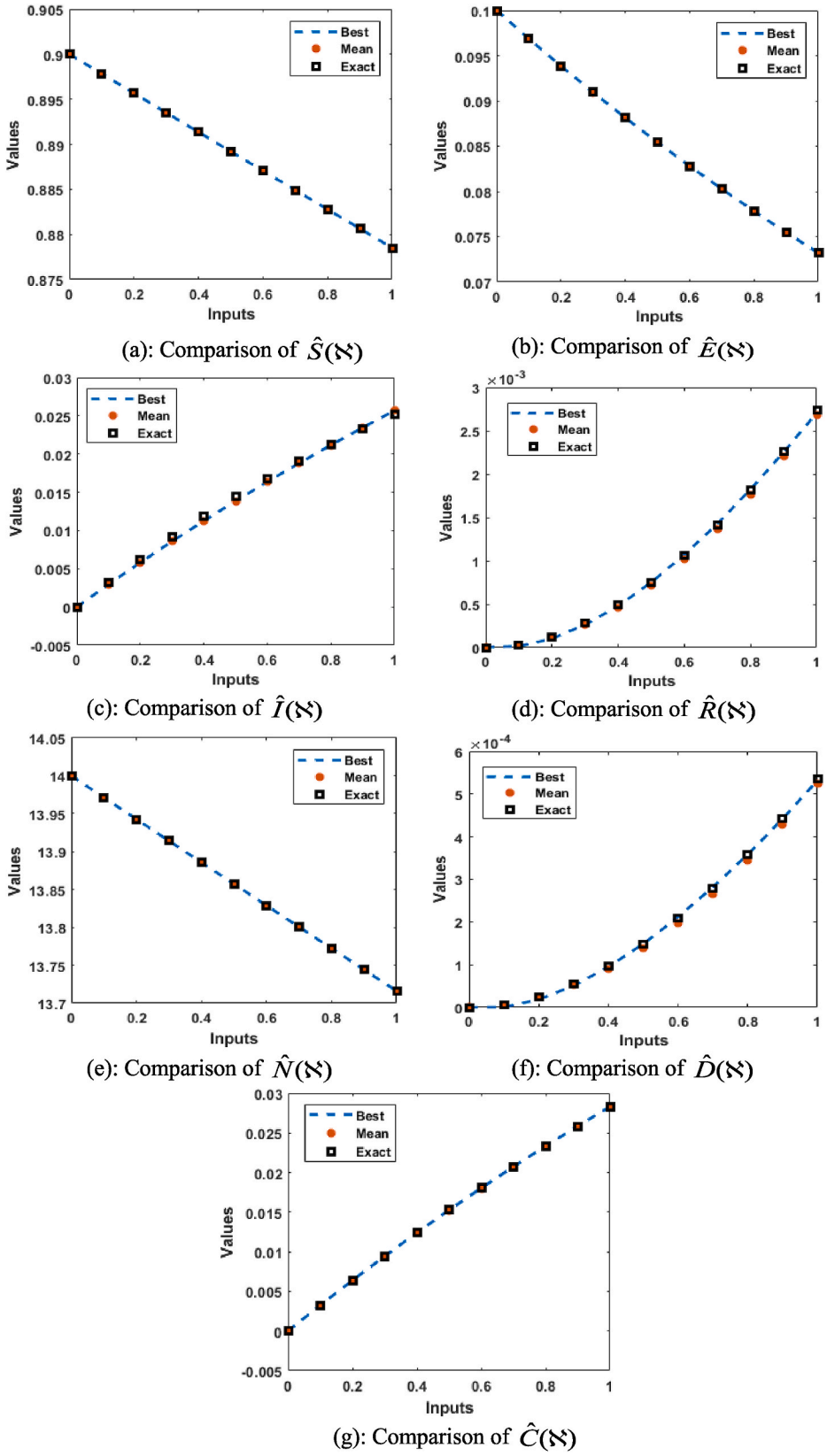

Fig. 3. Result comparison for the nonlinear SEIR-NDC model.

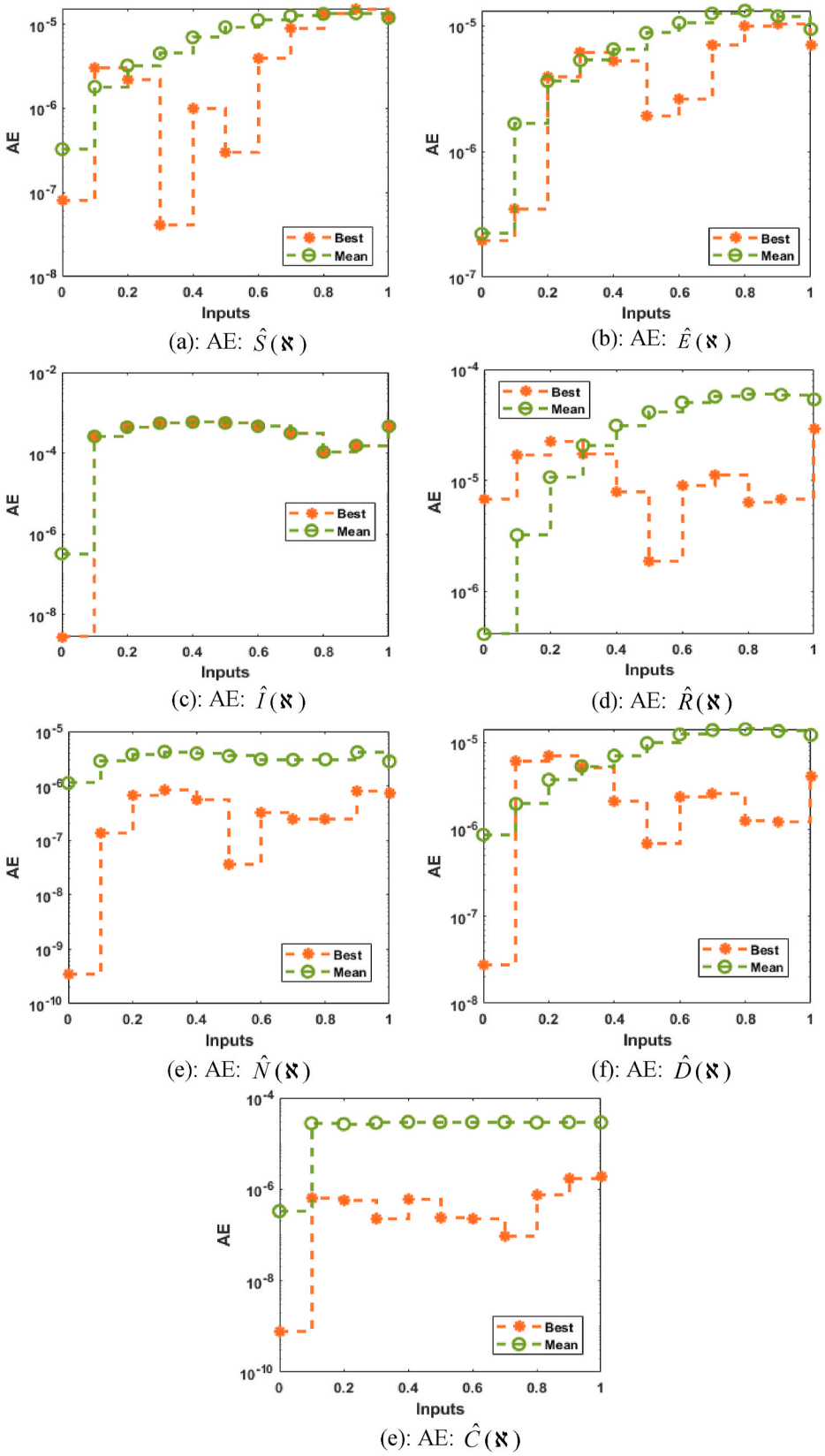

Fig. 4. Best/Mean AE for the nonlinear SEIR-NDC model.

3. Performance catalogues

In this section, the mathematical performances of VAF, TIC and MAD are provided for the SEIR-NDC model that is written as:

4. Results and discussion

This section provides detailed results and discussions for the nonlinear SEIR-NDC model. The comparative investigations using the reference solutions label the accuracy of the ANNs along with the optimization procedures of GA-ASA. Moreover, statistical valuations prompt the accuracy of the ANNs along with the stochastic performances of the SEIR-NDC model.

$$\begin{cases} \frac{dS(\aleph)}{d\aleph} = -\frac{0.5E(\aleph)S(\aleph)}{N} - \frac{0.6I(\aleph)S(\aleph)}{N} - 0.0205S(\aleph), S(0) = 0.9, \\ \frac{dE(\aleph)}{d\aleph} = \frac{0.5E(\aleph)S(\aleph)}{N} + \frac{0.6I(\aleph)S(\aleph)}{N} - \left(\frac{1}{3} + 0.0205\right)E(\aleph), E(0) = 0.1, \\ \frac{dI(\aleph)}{d\aleph} = \frac{1}{3}E(\aleph) - \left(\frac{1}{5} + 0.025\right)I(\aleph), I(0) = 0, \\ \frac{dR(\aleph)}{d\aleph} = -0.025R(\aleph) + \frac{1}{5}I(\aleph), R(0) = 0, \\ \frac{dN(\aleph)}{d\aleph} = -0.0205N(\aleph),\ N(0) = 14, \\ \frac{dD(\aleph)}{d\aleph} = -\frac{1}{11.2}D(\aleph) + 0.04I(\aleph), D(0) = 0, \\ \frac{dC(\aleph)}{d\aleph} = \frac{1}{3}E(\aleph), C(0) = 0. \end{cases} \tag{16}$$

The error function is given:

$$\xi_F = \frac{1}{N}\sum_{k=1}^{N}\left(\begin{array}{l} \left[\frac{d\widehat{S}}{d\aleph_k} + \frac{0.5\widehat{E}_k\widehat{S}_k}{N} + \frac{0.6\widehat{I}_k\widehat{S}_k}{N} + 0.0205\widehat{S}_k\right]^2 + \\ \left[\frac{d\widehat{E}}{d\aleph_k} - \frac{0.5\widehat{E}_k\widehat{S}_k}{N} - \frac{0.6\widehat{I}_k\widehat{S}_k}{N} + 0.3505\widehat{E}_k\right]^2 + \\ \left[\frac{d\widehat{I}}{d\aleph_k} - \frac{1}{3}\widehat{E}_k + 0.225\widehat{I}_k\right]^2 + \left[\frac{d\widehat{R}}{d\aleph_k} - \frac{1}{5}\widehat{I}_k + 0.025\widehat{R}_k\right]^2 \\ \left[\frac{d\widehat{N}}{d\aleph_k} + 0.0205\widehat{N}_k\right]^2 + \left[\frac{d\widehat{D}}{d\aleph_k} - 0.04\widehat{I}_k + \frac{1}{11.2}\widehat{D}_k\right]^2 + \left[\frac{d\widehat{C}}{d\aleph_k} - 0.33\widehat{E}_k\right]^2 \end{array}\right) + \frac{1}{7}\left(\begin{array}{l} (\widehat{S}_0 - 0.9)^2 + (\widehat{E}_0 - 0.1)^2 \\ +(\widehat{I}_0)^2 + (\widehat{R}_0)^2 + (\widehat{N}_0 - 14)^2 \\ +(\widehat{D}_0)^2 + (\widehat{C}_0)^2 \end{array}\right). k = 1$$

4.1. SEIR-NDC mathematical model

The simplified form of the nonlinear SEIR-NDC model using the suitable parameter values is given:

The optimization is performed to solve the SEIR-NDC system for 20 independent executions together with 30 or ten neurons (see Fig. 1). The best weight set values through ANNs using the hybrid optimization procedures are plotted in Fig. 2. These weights are proficient in finding the solutions of the SEIR-NDC system, given as [17].

$$\begin{aligned} \widehat{S}(\aleph) = {} & \frac{-0.6133}{1+e^{-(-0.5832\tau-3.3229)}} + \frac{0.1280}{1+e^{-(1.4989\tau-1.8666)}} + \frac{0.2820}{1+e^{-(-0.9587\tau04.1986)}} + \frac{1.5545}{1+e^{-(1.9321\tau+5.0796)}} \\ & + \frac{1.2002}{1+e^{-(0.7224\tau+4.5569)}} + \frac{0.3390}{1+e^{-(-0.1071\tau+3.0991)}} - \frac{0.5569}{1+e^{-(0.1025\tau+3.4372)}} + \frac{0.9118}{1+e^{-(-1.5653\tau+3.4393)}} \\ & + \frac{3.0917}{1+e^{-(0.2921\tau-5.1439)}} + \frac{0.5054}{1+e^{-(0.2505\tau+3.1504)}}, \end{aligned} \tag{18}$$

$$\begin{aligned} \widehat{E}(\aleph) = {} & \frac{-0.0682}{1+e^{-(-0.3121\tau+0.65155)}} + \frac{0.6531}{1+e^{-(1.3823\tau+2.1107)}} + \frac{-0.0437}{1+e^{-(-0.3316\tau+0.3945)}} + \frac{0.3931}{1+e^{-(-0.0854\tau-0.0814)}} \\ & - \frac{0.0473}{1+e^{-(-1.1772\tau+1.3201)}} - \frac{0.0132}{1+e^{-(-2.5078\tau-1.1537)}} - \frac{0.1398}{1+e^{-(2.1805\tau+2.1697)}} + \frac{-0.0979}{1+e^{-(-0.8542\tau+0.1619)}} \\ & - \frac{0.0357}{1+e^{-(-0.2550\tau+1.0518)}} + \frac{-0.1977}{1+e^{-(1.3348\tau+1.2213)}}, \end{aligned} \tag{19}$$

$$\begin{aligned} \widehat{I}(\aleph) = {} & \frac{0.1338}{1+e^{-(-0.0698\tau+0.7675)}} + \frac{0.4057}{1+e^{-(0.3161\tau-0.3940)}} - \frac{0.5275}{1+e^{-(0.8837\tau+0.7627)}} - \frac{0.0413}{1+e^{-(0.3452\tau+0.6267)}} \\ & - \frac{0.4058}{1+e^{-(-0.9279\tau-0.4624)}} - \frac{0.6059}{1+e^{-(0.2099\tau-0.0348)}} + \frac{1.0916}{1+e^{-(0.2073\tau+1.3967)}} + \frac{0.0045}{1+e^{-(0.6294\tau+0.6236)}} \\ & - \frac{0.0554}{1+e^{-(1.0184\tau-2.2828)}} + \frac{0.4776}{1+e^{-(0.4695\tau+0.4474)}}, \end{aligned} \tag{20}$$

$$\widehat{R}(\aleph) = \frac{-0.3678}{1+e^{-(1.4663\tau-0.4560)}} - \frac{-0.2632}{1+e^{-(0.5081\tau-2.3893)}} - \frac{0.0450}{1+e^{-(-1.2729\tau+0.6974)}} + \frac{-0.4095}{1+e^{-(1.2506\tau+0.9080)}} - \frac{0.1326}{1+e^{-(0.0612\tau+0.9015)}} - \frac{0.4787}{1+e^{-(0.1425\tau+1.0183)}} + \frac{2.1786}{1+e^{-(0.5785\tau+2.8092)}} - \frac{-0.1362}{1+e^{-(-1.5902\tau-0.1538)}} - \frac{0.3772}{1+e^{-(-0.4922\tau+0.2080)}} - \frac{0.1517}{1+e^{-(0.627\tau-0.2205)}}, \tag{21}$$

$$\widehat{N}(\aleph) = \frac{6.7406}{1+e^{-(0.2651\tau-3.8195)}} - \frac{-4.1033}{1+e^{-(-0.6517\tau+4.8271)}} - \frac{-1.3444}{1+e^{-(1.3935\tau-4.0924)}} - \frac{-5.1724}{1+e^{-(-2.0324\tau-4.1716)}} - \frac{0.2942}{1+e^{-(-0.6685\tau+1.6615)}} - \frac{-2.1599}{1+e^{-(0.4509\tau-2.0840)}} + \frac{3.8193}{1+e^{-(0.6905\tau+4.6065)}} - \frac{-1.0274}{1+e^{-(0.5341\tau+1.0892)}} + \frac{2.5149}{1+e^{-(1.2765\tau-3.8873)}} + \frac{2.0020}{1+e^{-(2.4318\tau+4.0372)}}, \tag{22}$$

$$\widehat{D}(\aleph) = \frac{-0.2389}{1+e^{-(1.4207\tau-1.4166)}} + \frac{0.1457}{1+e^{-(-0.4142\tau+1.2958)}} - \frac{0.0314}{1+e^{-(0.6556\tau+07408)}} - \frac{0.1308}{1+e^{-(-0.1415\tau+1.5052)}} - \frac{-0.4512}{1+e^{-(0.9756\tau+1.2410)}} - \frac{0.4132}{1+e^{-(-0.3249\tau+0.0923)}} + \frac{0.0018}{1+e^{-(-1.2983\tau+1.8050)}} + \frac{-0.5563}{1+e^{-(-0.2037\tau-0.3054)}} - \frac{-0.2565}{1+e^{-(0.3560\tau-0.0735)}} + \frac{-0.1085}{1+e^{-(1.0535\tau-0.2857)}}, \tag{23}$$

$$\widehat{C}(\aleph) = \frac{-1.0626}{1+e^{-(-1.1053\tau-1.2497)}} - \frac{0.3047}{1+e^{-(0.4213\tau+1.2013)}} - \frac{0.2253}{1+e^{-(0.9289\tau+1.1043)}} + \frac{-0.9582}{1+e^{-(+0.0746\tau-2.3808)}} - \frac{-0.0415}{1+e^{-(-1.9014\tau-0.3182)}} - \frac{-0.0950}{1+e^{-(-0.5001\tau+0.4560)}} + \frac{1.2014}{1+e^{-(-0.9330\tau-1.7745)}} - \frac{-1.0485}{1+e^{-(-0.5047\tau-2.0290)}} - \frac{0.4295}{1+e^{-(-0.3070\tau-0.4550)}} - \frac{-0.2063}{1+e^{-(0.4876\tau+0.5047)}}. \tag{24}$$

The Systems (18–24) are derived to assess the outcomes of the SEIR-NDC system using the optimization procedures of the ANNs together with GA-ASA. The results are drawn in Figs. 2–4 based on the 30 variables or ten neurons. Fig. 2(a–g) depicts the best weights for the nonlinear SEIR-NDC model. The mean and best results comparison for solving the SEIR-NDC model are presented in Fig. 3(a–g). It is observed that the proposed, best, and mean solutions are overlapped for each category of the nonlinear SEIR-NDC system. Fig. 4 is drawn based on AE in terms of best and mean outcomes for the nonlinear SEIR-NDC model. One can observe that the best AE for the $\widehat{S}(\aleph)$, $\widehat{E}(\aleph)$, $\widehat{I}(\aleph)$, $\widehat{R}(\aleph)$, $\widehat{N}(\aleph)$, $\widehat{D}(\aleph)$ and $\widehat{C}(\aleph)$ classes of the SEIR-NDC system lie as 10^{-06}-10^{-08}, 10^{-05}-10^{-07}, 10^{-02}-10^{-04}, 10^{-04}-10^{-05}, 10^{-06}-10^{-08}, 10^{-05}-10^{-07} and 10^{-06} to 10^{-08}, respectively. The mean values for these respective dynamics of the SEIR-NDC system are calculated as 10^{-05}-10^{-07}, 10^{-05}-10^{-06},

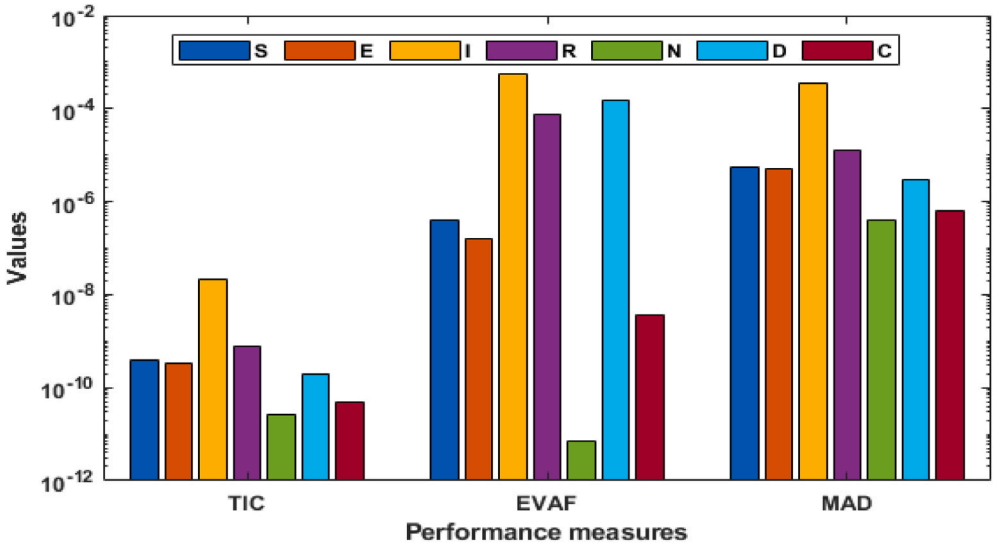

Fig. 5. Performance measures for the nonlinear SEIR-NDC model.

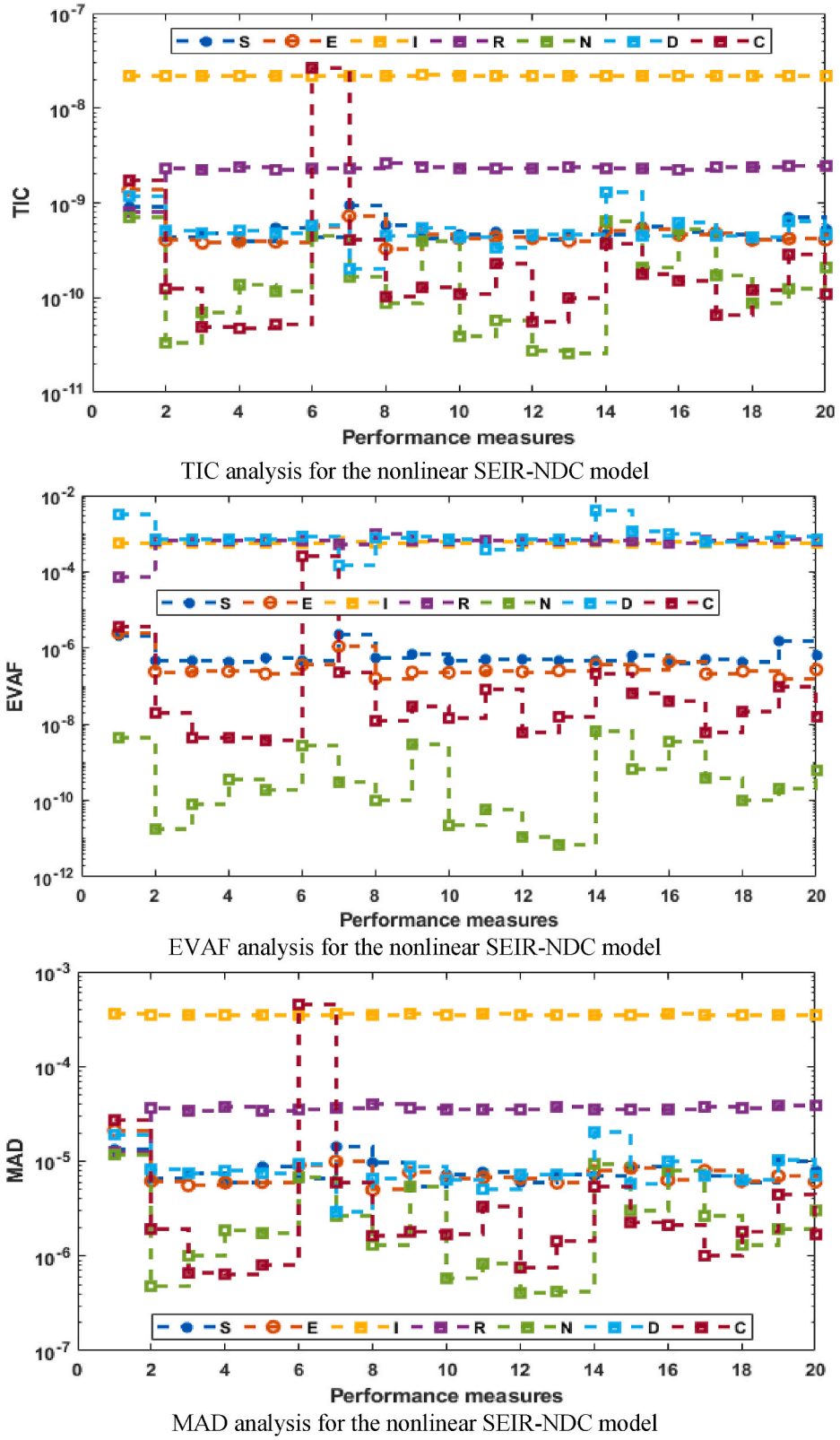

Fig. 6. Convergence of TIC, EVAF and MAD for the nonlinear SEIR-NDC model.

10^{-02}-10^{-06}, 10^{-05}-10^{-07}, 10^{-05}-10^{-06}, 10^{-04}-10^{-07} and 10^{-04}-10^{-06}. It is seen that the AE through the designed computational scheme is accurate in solving the nonlinear SEIR-NDC model. One can accomplish that the designed numerical procedure is accurate in terms of the AE.

The performances through the statistical TIC, EVAF and MAD operators are demonstrated in Fig. 5. It is indicated that the performances of TIC for the $\widehat{S}(\aleph)$, $\widehat{E}(\aleph)$, $\widehat{I}(\aleph)$, $\widehat{R}(\aleph)$, $\widehat{N}(\aleph)$, $\widehat{D}(\aleph)$ and $\widehat{C}(\aleph)$ lie around 10^{-08}-10^{-10}, 10^{-09}-10^{-10}, 10^{-07}-10^{-08}, 10^{-08}-10^{-10}, 10^{-11}-10^{-12}, 10^{-09}-10^{-10} and 10^{-10}-10^{-11}. The performance of EVAF for the respective dynamics of the SEIR-NDC model found 10^{-06}-10^{-07}, 10^{-07}-

Table 2
Statistics results of the nonlinear SEIR-NDC model for.$S(\aleph)$

$\aleph$	$S(\aleph)$					
	Min	Max	Mean	Median	S.I.R	STD
0	3.60032E-11	2.30688E-06	3.95126E-08	3.27227E-07	1.52327E-07	6.70737E-07
0.1	2.09410E-08	8.70303E-06	8.39999E-07	1.79962E-06	9.68586E-07	2.14007E-06
0.2	4.08596E-07	1.77019E-05	1.80603E-06	3.22998E-06	6.55853E-07	4.08677E-06
0.3	4.11253E-08	1.87691E-05	3.65699E-06	4.50105E-06	1.92684E-06	4.81840E-06
0.4	1.00314E-06	2.32212E-05	6.26634E-06	6.97651E-06	1.81048E-06	4.51337E-06
0.5	2.98064E-07	2.23982E-05	8.34863E-06	9.21741E-06	1.81457E-06	4.57419E-06
0.6	3.93181E-06	2.06716E-05	1.03632E-05	1.11690E-05	1.50990E-06	3.83299E-06
0.7	7.73273E-06	2.56817E-05	1.19012E-05	1.25365E-05	1.24511E-06	3.55931E-06
0.8	6.62059E-07	2.76447E-05	1.27180E-05	1.32761E-05	9.02358E-07	5.27729E-06
0.9	3.87578E-06	3.28068E-05	1.26747E-05	1.34751E-05	1.15532E-06	5.99386E-06
1	3.84973E-06	2.75718E-05	1.14109E-05	1.19712E-05	8.16100E-07	4.50341E-06

Table 3
Statistics results of the nonlinear SEIR-NDC model for.$E(\aleph)$

$\aleph$	$E(\aleph)$ $A_h(\chi)$					
	Min	Max	Mean	Median	S.I.R	STD
0	6.88809E-10	2.10246E-06	7.62645E-08	2.21527E-07	1.01650E-07	4.67928E-07
0.1	7.49512E-08	1.60480E-05	5.09385E-07	1.66523E-06	2.88441E-07	3.57085E-06
0.2	3.15757E-07	2.66627E-05	1.98827E-06	3.63804E-06	1.33269E-06	5.63233E-06
0.3	9.48688E-07	2.03071E-05	4.20348E-06	5.32163E-06	2.15614E-06	4.23606E-06
0.4	2.16166E-06	1.20152E-05	6.06888E-06	6.52171E-06	2.14547E-06	2.87345E-06
0.5	1.93589E-06	1.89592E-05	7.60552E-06	8.80009E-06	1.59389E-06	3.77635E-06
0.6	1.64671E-07	3.56753E-05	9.56830E-06	1.05852E-05	1.21693E-06	6.80060E-06
0.7	7.01474E-06	4.31385E-05	1.09666E-05	1.25809E-05	9.70676E-07	7.34798E-06
0.8	8.89149E-06	3.87457E-05	1.14043E-05	1.32153E-05	6.20230E-07	6.70759E-06
0.9	5.69500E-06	2.76896E-05	1.04845E-05	1.19431E-05	8.13679E-07	4.81023E-06
1	6.51409E-06	1.79725E-05	8.85306E-06	9.43398E-06	8.88891E-07	2.52373E-06

Table 4
Statistics results of the nonlinear SEIR-NDC model for.$I(\aleph)$

$\aleph$	$I(\aleph)$ $A_h(\chi)$					
	Min	Max	Mean	Median	S.I.R	STD
0	1.13711E-10	2.84983E-06	3.85940E-08	3.21677E-07	1.35843E-07	6.89181E-07
0.1	2.56215E-04	2.71479E-04	2.59523E-04	2.60247E-04	8.52226E-07	3.46002E-06
0.2	4.36681E-04	4.56616E-04	4.41761E-04	4.43102E-04	1.17234E-06	4.30802E-06
0.3	5.45026E-04	5.62898E-04	5.50013E-04	5.51683E-04	2.89995E-06	4.53615E-06
0.4	5.84565E-04	5.99582E-04	5.87136E-04	5.89382E-04	3.28600E-06	4.61257E-06
0.5	5.55910E-04	5.68026E-04	5.57382E-04	5.59677E-04	1.74146E-06	3.99099E-06
0.6	4.60442E-04	4.75154E-04	4.65838E-04	4.66607E-04	1.53037E-06	3.52522E-06
0.7	3.04993E-04	3.19985E-04	3.14695E-04	3.14234E-04	1.25718E-06	3.18414E-06
0.8	9.50511E-05	1.09362E-04	1.07102E-04	1.06356E-04	5.74370E-07	3.14357E-06
0.9	1.41975E-04	1.65273E-04	1.52984E-04	1.53684E-04	1.64303E-06	4.22739E-06
1	4.52250E-04	4.72026E-04	4.63375E-04	4.63114E-04	9.81812E-07	3.52136E-06

Table 5
Statistics results of the nonlinear SEIR-NDC model for.$R(\aleph)$

$\aleph$	$R(\aleph)$ $A_h(\chi)$					
	Min	Max	Mean	Median	S.I.R	STD
0	6.69144E-11	6.76242E-06	2.49468E-08	4.13129E-07	6.56059E-08	1.49924E-06
0.1	1.56388E-07	1.70055E-05	2.79619E-06	3.22756E-06	6.25032E-07	3.39717E-06
0.2	5.54984E-06	2.23443E-05	1.01927E-05	1.07093E-05	1.58972E-06	3.59795E-06
0.3	1.72329E-05	2.63359E-05	1.96740E-05	2.06821E-05	2.08094E-06	3.04426E-06
0.4	7.94102E-06	3.91228E-05	3.14578E-05	3.13013E-05	1.69664E-06	6.24737E-06
0.5	1.87792E-06	5.06177E-05	4.30155E-05	4.13918E-05	1.44107E-06	9.68471E-06
0.6	8.99977E-06	5.96879E-05	5.19618E-05	5.04315E-05	9.06125E-07	1.01120E-05
0.7	1.10951E-05	6.94103E-05	5.85033E-05	5.68530E-05	1.25266E-06	1.11715E-05
0.8	6.33613E-06	7.38015E-05	6.27220E-05	5.99176E-05	1.53876E-06	1.30255E-05
0.9	6.73912E-06	7.11628E-05	6.14471E-05	5.91862E-05	1.72105E-06	1.28110E-05
1	2.93008E-05	5.98895E-05	5.49934E-05	5.36986E-05	1.68790E-06	6.21892E-06

Table 6
Statistics results of the nonlinear SEIR-NDC model for.$N(\aleph)$

$\aleph$	$N(\aleph)$ $A_h(\chi)$					
	Min	Max	Mean	Median	S.I.R	STD
0	4.22933E-11	1.59967E-05	7.05358E-08	1.12599E-06	2.03306E-07	3.55582E-06
0.1	1.36108E-07	1.81456E-05	9.01977E-07	2.85176E-06	8.03353E-07	4.71349E-06
0.2	1.33456E-07	1.79176E-05	2.20318E-06	3.73526E-06	2.11311E-06	4.70232E-06
0.3	1.42898E-07	1.28182E-05	2.77591E-06	4.21140E-06	2.55727E-06	3.62734E-06
0.4	1.78081E-07	2.02060E-05	2.66575E-06	3.93302E-06	2.04317E-06	4.68974E-06
0.5	3.67748E-08	2.17867E-05	1.56158E-06	3.51696E-06	1.83709E-06	5.41211E-06
0.6	5.99113E-08	1.70662E-05	1.01354E-06	3.06191E-06	9.14093E-07	5.10185E-06
0.7	1.90916E-08	1.80211E-05	1.02757E-06	2.99907E-06	2.13178E-06	4.44307E-06
0.8	1.21499E-07	1.73111E-05	1.13196E-06	3.04855E-06	9.62549E-07	4.85588E-06
0.9	3.65011E-07	1.55190E-05	2.52975E-06	4.13153E-06	1.97983E-06	4.32362E-06
1	6.93436E-08	1.03581E-05	1.87436E-06	2.79862E-06	2.04956E-06	2.96112E-06

Table 7
Statistics results of the nonlinear SEIR-NDC model for.$D(\aleph)$

$\aleph$	$D(\aleph)$ $A_h(\chi)$					
	Min	Max	Mean	Median	S.I.R	STD
0	1.10686E-10	1.10597E-05	2.10310E-08	8.65604E-07	8.70769E-08	2.57431E-06
0.1	1.02404E-07	1.58579E-05	8.49577E-07	1.96336E-06	4.55001E-07	3.59481E-06
0.2	1.57822E-07	1.30637E-05	2.91483E-06	3.70358E-06	1.59103E-06	2.93113E-06
0.3	3.43656E-07	1.53426E-05	4.70454E-06	5.29591E-06	1.12594E-06	3.24657E-06
0.4	1.07689E-07	2.45192E-05	6.07023E-06	6.99999E-06	1.63718E-06	5.25789E-06
0.5	6.78080E-07	3.10306E-05	8.45347E-06	9.74805E-06	1.95175E-06	6.23115E-06
0.6	2.38683E-06	3.35138E-05	1.04739E-05	1.22721E-05	2.12751E-06	6.60005E-06
0.7	2.58242E-06	3.20802E-05	1.20257E-05	1.37990E-05	1.48098E-06	6.65682E-06
0.8	1.24887E-06	3.38603E-05	1.29028E-05	1.41286E-05	8.45757E-07	6.56672E-06
0.9	1.21663E-06	3.18514E-05	1.28942E-05	1.34596E-05	1.37818E-06	6.24252E-06
1	3.16966E-06	2.54620E-05	1.15257E-05	1.21126E-05	1.35198E-06	5.21726E-06

Table 8
Statistics results of the nonlinear SEIR-NDC model for.$C(\aleph)$

$\aleph$	$C(\aleph)$ $A_h(\chi)$					
	Min	Max	Mean	Median	S.I.R	STD
0	3.90810E-11	4.23918E-06	1.35893E-08	3.31828E-07	7.62130E-08	9.55850E-07
0.1	5.62845E-08	5.39600E-04	4.44063E-07	2.79071E-05	3.90929E-07	1.20452E-04
0.2	1.51668E-07	5.00345E-04	1.23355E-06	2.67422E-05	1.26634E-06	1.11486E-04
0.3	3.87496E-08	5.00317E-04	3.18914E-06	2.86553E-05	2.10489E-06	1.11072E-04
0.4	2.15256E-07	4.97742E-04	3.22013E-06	2.98108E-05	2.43583E-06	1.10297E-04
0.5	1.36397E-07	5.00520E-04	3.44456E-06	2.97193E-05	2.61805E-06	1.11135E-04
0.6	2.20479E-07	5.03994E-04	1.54931E-06	2.94355E-05	1.51904E-06	1.12172E-04
0.7	9.23625E-08	5.05010E-04	1.53333E-06	2.95272E-05	1.16646E-06	1.12428E-04
0.8	4.11928E-07	5.03711E-04	1.32369E-06	2.88498E-05	9.23804E-07	1.12209E-04
0.9	1.65679E-07	5.01960E-04	2.08305E-06	2.92883E-05	1.22298E-06	1.11559E-04
1	3.10505E-07	5.02207E-04	1.98610E-06	2.90106E-05	1.39515E-06	1.11553E-04

10^{-08}, 10^{-03}-10^{-04}, 10^{-04}-10^{-05}, 10^{-11}-10^{-12}, 10^{-04}-10^{-05} and 10^{-09}-10^{-10}, respectively. The performance of MAD $\widehat{S}(\aleph)$, $\widehat{E}(\aleph)$, $\widehat{I}(\aleph)$, $\widehat{R}(\aleph)$, $\widehat{N}(\aleph)$, $\widehat{D}(\aleph)$ and $\widehat{C}(\aleph)$ also found in good ranges. These optimal small measures improve the worth and accuracy of the stochastic scheme.

Fig. 6 shows the analysis of TIC, EVAF and MAD operator for the nonlinear SEIR-NDC model. It is observed through these analyses that most of the runs achieve good fitness levels. One can accomplish that the designed approach is stable and reliable.

To check the precision, accuracy, and correctness of the designed scheme, the statistical depictions based on the SEIR-NDC system are derived in Tables 2 - 8 for the $\widehat{S}(\aleph)$, $\widehat{E}(\aleph)$, $\widehat{I}(\aleph)$, $\widehat{R}(\aleph)$,$\widehat{N}(\aleph)$, $\widehat{D}(\aleph)$ and $\widehat{C}(\aleph)$. The statistical outcomes for the operators Maximum (Max), Minimum (Min), semi-interquartile range (SIR), Median, Mean and standard deviation (STD) are presented. The Min and Max values represent the best and bad trials, while S.I.R is one-half of the difference between the 3rd and first quartiles. One can observe that the Min operator values of $\widehat{S}(\aleph)$, $\widehat{E}(\aleph)$, $\widehat{I}(\aleph)$, $\widehat{R}(\aleph)$,$\widehat{N}(\aleph)$, $\widehat{D}(\aleph)$ and $\widehat{C}(\aleph)$ found as 10^{-06}-10^{-11}, 10^{-06}-10^{-10}, 10^{-04}-10^{-10}, 10^{-05}-10^{-11}, 10^{-07}-10^{-11} and 10^{-06}-10^{-10}. The Max operator values that indicate the worst trials were found around 10^{-05}-10^{-06} for each category of the SEIR-NDC system. The S.I.R, Mean and STD and Median values of the statistics lie as 10^{-06}-10^{-08} for each dynamic of the SEIR-NDC system. These calculated values indicate the reliability of the proposed scheme to solve the SEIR-NDC model.

5. Concluding remarks

This work aims to solve the SEIR-NDC nonlinear model using the strength of artificial neural networks and the optimization procedures of genetic algorithms and active-set techniques. The SEIR-NDC-based COVID-19 nonlinear mathematical model has never been solved using

the stochastic approaches based on the GA-ASA. The validation of the proposed ANNs through the optimization of GA-ASA is observed by using the comparison of the reference and obtained results. It is noticed that the absolute error is found in good measures that are calculated as 10-07 to 10-10 for each dynamic of the SEIR-NDC system. The absolute error values are also authenticated in good measures for solving the nonlinear SEIR-NDC mathematical model.

Furthermore, the operator's TIC, EVAF, and MAD performances have been examined in good procedures for 30 numbers of variables to solve the SEIR-NDC nonlinear model. Moreover, the statistical-based operator's Min, Max, S.I.R. Mean, Median, and STD are in good ranges for solving the nonlinear SEIR-NDC nonlinear mathematical model. It is proved through these witnesses that the designed scheme is reliable, stable, robust, and accurate for solving the nonlinear SIER-NDC mathematical model.

Future research directions

the proposed stochastic computing framework can be applied to solve the nonlinear mathematical models arising in fluid dynamics [54–57], thermal explosion models [58,59], singular studies [60,61], and food chain systems [62,63].

Declaration of competing interest

The authors declare that they have no known competing financial interests or personal relationships that could have appeared to influence the work reported in this paper.

Acknowledgements

This project was supported financially by the Academy of Scientific Research & Technology (ASRT), Egypt. Grant No. 6436 under the project ScienceUp. (ASRT) is the 2nd affiliation of this research.

References

[1] Ramani VK, et al. A study on the global scenario of COVID-19 related case fatality rate, recovery rate and prevalence rate and its implications for India—a record based retrospective cohort study. Adv Infect Dis 2020;10(3):233–48.
[2] Zaim S, Chong JH, Sankaranarayanan V, Harky A. COVID-19 and multiorgan response. Curr Probl Cardiol 2020;45(8):100618.
[3] Umar M, et al. A stochastic intelligent computing with neuro-evolution heuristics for nonlinear SITR system of novel COVID-19 dynamics. Symmetry 2020;12(10):1628.
[4] Covid C, Team R, Jorden MA, Rudman SL, Villarino E, Hoferka S, Patel MT, Bemis K, Simmons CR, Jespersen M, Johnson JI. Evidence for limited early spread of COVID-19 within the United States, January–February 2020. MMWR (Morb Mortal Wkly Rep) 2020;69(22):680.
[5] Botmart T, et al. A numerical study of the fractional order dynamical nonlinear susceptible infected and quarantine differential model using the stochastic numerical approach. Fractal and Fractional 2022;6(3):139.
[6] May Pratiwi CD, et al. Euler's and Heun's numerical solutions to a mathematical model of the spread of COVID-19. In: AIP conference proceedings, vol. 2353. AIP Publishing LLC; 2021, 030110. No. 1.
[7] Weng LM, Su X, Wang XQ. Pain symptoms in patients with coronavirus disease (COVID-19): a literature review. J Pain Res 2021;14:147.
[8] Zare-Zardini H, Soltaninejad H, Ferdosian F, Hamidieh AA, Memarpoor-Yazdi M. Coronavirus disease 2019 (COVID-19) in children: prevalence, diagnosis, clinical symptoms, and treatment. Int J Gen Med 2020;13:477.
[9] Sabir Z, Alnahdi AS, Jeelani MB, Abdelkawy MA, Raja MAZ, Baleanu D, Hussain MM. Numerical computational heuristic through morlet wavelet neural network for solving the dynamics of nonlinear SITR COVID-19. Cmes-Computer Modeling in Engineering & Sciences; 2022. p. 763–85.
[10] Donders F, et al. ISIDOG recommendations concerning COVID-19 and pregnancy. Diagnostics 2020;10(4):243.
[11] Wang J. Mathematical models for COVID-19: applications, limitations, and potentials. J Publ Health Epidemiol 2020;4.
[12] Rhodes T, et al. Mathematical models as public troubles in COVID-19 infection control: following the numbers. Health Sociol Rev 2020;29(2):177–94.
[13] Jewell BL, et al. Potential effects of disruption to HIV programmes in sub-Saharan Africa caused by COVID-19: results from multiple mathematical models. The Lancet HIV 2020;7(9):e629–40.
[14] Khrapov P, et al. Comparative analysis of the mathematical models of the dynamics of the coronavirus COVID-19 epidemic development in the different countries. Int J Open Inf Technol 2020;8(5):17–22.
[15] Thompson RN. Epidemiological models are important tools for guiding COVID-19 interventions. BMC Med 2020;18:1–4.
[16] Sánchez YG, et al. Design of a nonlinear SITR fractal model based on the dynamics of a novel coronavirus (COVID-19). Fractals 2020;28:2040026. 08.
[17] Elsonbaty A, et al. Dynamical analysis of a novel discrete fractional SITRs model for COVID-19. 2021, 2140035. Fractals.
[18] Umar M, et al. A stochastic intelligent computing with neuro-evolution heuristics for nonlinear SITR system of novel COVID-19 dynamics. Symmetry 2020;12(10):1628.
[19] Umar M, et al. Integrated neuro-swarm heuristic with interior-point for nonlinear SITR model for dynamics of novel COVID-19. Alex Eng J 2021;60(3):2811–24.
[20] Side S, et al. Stability analysis susceptible, exposed, infected, recovered (SEIR) model for spread of dengue fever in Medan. Statistics, Mathematics, Teaching, and Research 2015:246.
[21] Hidayat MHP, et al. Leksikon penyair kalimantan selatan (1930–2020). 2020.
[22] Sabir Z, et al. Solving a novel designed second order nonlinear Lane–Emden delay differential model using the heuristic techniques. Appl Soft Comput 2021;102:107105.
[23] Guirao JL, et al. Design and numerical solutions of a novel third-order nonlinear Emden–Fowler delay differential model. Math Probl Eng 2020;2020. 2020.
[24] Umar M, et al. Intelligent computing for numerical treatment of nonlinear prey–predator models. Appl Soft Comput 2019;80:506–24.
[25] Sabir Z, et al. A novel design of fractional Meyer wavelet neural networks with application to the nonlinear singular fractional Lane-Emden systems. Alex Eng J 2021;60(2):2641–59.
[26] Sabir Z, et al. Fractional Mayer Neuro-swarm heuristic solver for multi-fractional Order doubly singular model based on Lane-Emden equation. 2021. Fractals.
[27] Sabir Z, et al. FMNEICS: fractional Meyer neuro-evolution-based intelligent computing solver for doubly singular multi-fractional order Lane–Emden system. Comput Appl Math 2020;39(4):1–18.
[28] Umar M, et al. Stochastic numerical technique for solving HIV infection model of CD4+ T cells. Eur Phys J Plus 2020;135(6):403.
[29] Umar M, Amin F, Wahab HA, Baleanu D. Unsupervised constrained neural network modeling of boundary value corneal model for eye surgery. Appl Soft Comput 2019;85:105826.
[30] Wang B, et al. Numerical computing to solve the nonlinear corneal system of eye surgery using the capability of Morlet wavelet artificial neural networks. 2022, 2240147. Fractals.
[31] Sabir Z, et al. Neuro-swarm intelligent computing to solve the second-order singular functional differential model. Eur Phys J Plus 2020;135(6):474.
[32] Sabir Z, et al. Neuro-heuristics for nonlinear singular Thomas-Fermi systems. Appl Soft Comput 2018;65:152–69.
[33] Umar M, et al. A stochastic computational intelligent solver for numerical treatment of mosquito dispersal model in a heterogeneous environment. Eur Phys J Plus 2020;135(7):1–23.
[34] Raja MAZ, et al. A new stochastic computing paradigm for the dynamics of nonlinear singular heat conduction model of the human head. Eur Phys J Plus 2018;133(9):364.
[35] Sabir Z, et al. Evolutionary computing for nonlinear singular boundary value problems using neural network, genetic algorithm and active-set algorithm. Eur Phys J Plus 2021;136(2):1–19.
[36] Sabir Z, et al. A neuro-swarming intelligence-based computing for second order singular periodic non-linear boundary value problems. Front Physiol 2020;8:224.
[37] May Pratiwi CD, et al. Euler's and Heun's numerical solutions to a mathematical model of the spread of COVID-19. In: AIP conference proceedings, vol. 2353. AIP Publishing LLC; 2021, 030110. No. 1.
[38] Umar M, Amin F, Al-Mdallal Q, Ali MR. A stochastic computing procedure to solve the dynamics of prevention in HIV system. Biomed Signal Process Control 2022;78:103888.
[39] Sabir Z, et al. Designing of Morlet wavelet as a neural network for a novel prevention category in the HIV system. Int J Biomath (IJB) 2022;15:2250012. 04.
[40] Maleki N, et al. A k-NN method for lung cancer prognosis with the use of a genetic algorithm for feature selection. Expert Syst Appl 2021;164:113981.
[41] Rohani Y, Torabi Z, Kianian S. A novel hybrid genetic algorithm to predict students' academic performance. J Electr Comput Eng Innovat 2020;8(2):219–32.
[42] Liang H, Zou J, Zuo K, Khan MJ. An improved genetic algorithm optimization fuzzy controller applied to the wellhead back pressure control system. Mech Syst Signal Process 2020;142:106708.
[43] Jatana N, Suri B. Particle swarm and genetic algorithm applied to mutation testing for test data generation: a comparative evaluation. J King Saud Univ Comput Inf Sci. 2020;32(4):514–21.
[44] Toma RN, Prosvirin AE, Kim JM. Bearing fault diagnosis of induction motors using a genetic algorithm and machine learning classifiers. Sensors 2020;20(7):1884.
[45] Apornak A, Raissi S, Keramati A, Khalili-Damghani K. Human resources optimization in hospital emergency using the genetic algorithm approach. Int J Healthc Manag 2020:1–8.
[46] Chen F, Xu S, Zhao Y, Zhang H. An adaptive genetic algorithm of adjusting sensor acquisition frequency. Sensors 2020;20(4):990.
[47] Sabir Z, Amin F, Pohl D, Guirao JL. Intelligence computing approach for solving second order system of Emden–Fowler model. J Intell Fuzzy Syst 2020:1–16.
[48] Zan X, Wu Z, Guo C, Yu Z. A Pareto-based genetic algorithm for multi-objective scheduling of automated manufacturing systems. Adv Mech Eng 2020;12(1):1687814019885294.

[49] Li Y, Yuan G, Sheng Z. An active-set algorithm for solving large-scale nonsmooth optimization models with box constraints. PLoS One 2018;13(1):e0189290.
[50] Chamakuri N, Kunisch K. Primal-dual active set strategy for large scale optimization of cardiac defibrillation. Appl Math Comput 2017;292:178–93.
[51] Burdakov O, Sysoev O. A dual active-set algorithm for regularized monotonic regression. J Optim Theor Appl 2017;172(3):929–49.
[52] Nak, H., Akkaya, Ş. and Yumuk, E., Active set method based model predictive control for a ball and beam system. In 2017 10th international conference on electrical and electronics engineering (ELECO) (pp. 871-875). IEEE.
[53] Gilbert AD, Wasilkowski GW. Small superposition dimension and active set construction for multivariate integration under modest error demand. J Complex 2017;42:94–109.
[54] Sabir Z, Imran A, Umar M, Zeb M, Shoaib M, Raja MAZ. A numerical approach for 2-D Sutterby fluid-flow bounded at a stagnation point with an inclined magnetic field and thermal radiation impacts. Therm Sci 2021;25:1975–87. 3 Part A.
[55] Eskitaşçıoğlu Eİ, Aktaş MB, Baskonus HM. New complex and hyperbolic forms for Ablowitz–Kaup–Newell–Segur wave equation with fourth order. Appl Math Nonlinear Sci 2019;4(1):93–100.
[56] Sabir Z, Ayub A, Guirao JL, Bhatti S, Shah SZH. The effects of activation energy and thermophoretic diffusion of nanoparticles on steady micropolar fluid along with Brownian motion. Adv Mater Sci Eng 2020;2020. 2020.
[57] Kenway GK, Mader CA, He P, Martins JR. Effective adjoint approaches for computational fluid dynamics. Prog Aero Sci 2019;110:100542.
[58] Sabir Z. Neuron analysis through the swarming procedures for the singular two-point boundary value problems arising in the theory of thermal explosion. Eur Phys J Plus 2022;137(5):638.
[59] Sabir Z, Wahab HA, Ali MR, Sadat R. Neuron analysis of the two-point singular boundary value problems arising in the thermal explosion's theory. Neural Process Lett 2022:1–28.
[60] Sabir Z, Wahab HA. Evolutionary heuristic with Gudermannian neural networks for the nonlinear singular models of third kind. Phys Scripta 2021;96(12):125261.
[61] Sabir Z, Wahab HA, Javeed S, Baskonus HM. An efficient stochastic numerical computing framework for the nonlinear higher order singular models. Fractal and Fractional 2021;5(4):176.
[62] Sabir Z. Stochastic numerical investigations for nonlinear three-species food chain system. Int J Biomath (IJB) 2022;15:2250005. 04.
[63] Sabir Z, Ali MR, Sadat R. Gudermannian neural networks using the optimization procedures of genetic algorithm and active set approach for the three-species food chain nonlinear model. J Ambient Intell Hum Comput 2022:1–10.